Lymphatic function is required prenatally for lung inflation at birth

Zoltán Jakus,[1,2] Jason P. Gleghorn,[4] David R. Enis,[3] Aslihan Sen,[1,2] Stephanie Chia,[1,2] Xi Liu,[1,2,5] David R. Rawnsley,[1,2] Yiqing Yang,[1,2] Paul R. Hess,[1,2] Zhiying Zou,[1,2] Jisheng Yang,[1,2] Susan H. Guttentag,[6] Celeste M. Nelson,[4] and Mark L. Kahn[1,2]

[1]Department of Medicine, [2]Cardiovascular Institute, and [3]Department of Dermatology, University of Pennsylvania, Philadelphia, PA 19104
[4]Department of Chemical and Biological Engineering, Princeton University, Princeton, NJ 08544
[5]Fourth Military Medical University, Xi'an 710032, China
[6]Department of Neonatology, Children's Hospital of Philadelphia, Philadelphia, PA 19104

Mammals must inflate their lungs and breathe within minutes of birth to survive. A key regulator of neonatal lung inflation is pulmonary surfactant, a lipoprotein complex which increases lung compliance by reducing alveolar surface tension (Morgan, 1971). Whether other developmental processes also alter lung mechanics in preparation for birth is unknown. We identify prenatal lymphatic function as an unexpected requirement for neonatal lung inflation and respiration. Mice lacking lymphatic vessels, due either to loss of the lymphangiogenic factor CCBE1 or VEGFR3 function, appear cyanotic and die shortly after birth due to failure of lung inflation. Failure of lung inflation is not due to reduced surfactant levels or altered development of the lung but is associated with an elevated wet/dry ratio consistent with edema. Embryonic studies reveal active lymphatic function in the late gestation lung, and significantly reduced total lung compliance in late gestation embryos that lack lymphatics. These findings reveal that lymphatic vascular function plays a previously unrecognized mechanical role in the developing lung that prepares it for inflation at birth. They explain respiratory failure in infants with congenital pulmonary lymphangiectasia, and suggest that inadequate late gestation lymphatic function may also contribute to respiratory failure in premature infants.

CORRESPONDENCE
Mark L. Kahn:
markkahn@mail.med.upenn.edu

Abbreviation used: RDS, respiratory distress syndrome.

The most dramatic physiological change associated with birth is the onset of respiration. Mammals must breathe within minutes of birth to deliver oxygen to the brain and other organs, yet the lungs develop in a fluid environment and do not function until the time of birth. Successful neonatal respiration requires a complex prenatal lung maturation program that prepares the lung for air inflation and gas exchange at birth. A key aspect of this preparation is mechanical, i.e., increasing the compliance of the lung so that it can be successfully inflated at the time of birth (Guyton and Hall, 2000). A known regulator of pulmonary compliance is surfactant, a lipoprotein mixture produced in the late gestation lung that increases lung compliance by reducing alveolar surface tension (Avery and Mead, 1959; Adams et al., 1965; Morgan, 1971). The importance of prenatal lung maturation in neonatal respiration is revealed by the high incidence of respiratory failure, termed respiratory distress syndrome (RDS), among infants born before 29 wk of gestation (Hintz et al., 2005). Surfactant administration improves pulmonary compliance and RDS mortality (Couser et al., 1990), but premature infants still require supportive care such as oxygen and mechanical ventilation that are associated with long-term complications (Hintz et al., 2005; Suresh and Soll, 2005). The identification of additional mechanical aspects of lung maturation that may contribute to the pathogenesis of RDS is necessary to more effectively treat this common disease.

S.H. Guttentag's present address is Dept. of Pediatrics, Vanderbilt University, Nashville, TN 37232

The Rockefeller University Press $30.00
J. Exp. Med. 2014 Vol. 211 No. 5 815-826
www.jem.org/cgi/doi/10.1084/jem.20132308

The Journal of Experimental Medicine

The lymphatic vascular network is comprised of an open capillary system that drains fluid and proteins that have leaked from the high pressure blood vascular network into the interstitium. The prevention of tissue edema is considered a universal role of lymphatics and one that operates in a similar fashion and for a similar purpose in all tissues except the central nervous system, where a tight blood–brain barrier prevents fluid and protein leak. In addition to its global role in preventing tissue edema, lymphatic vessels are known to play specialized roles in coordinating adaptive immune responses in secondary lymphoid organs and in the transport of dietary lipids from the intestine (Tammela and Alitalo, 2010; Wang and Oliver, 2010). Whether lymphatic vessels play other organ-specific roles is not yet known.

In the present study, we examine the cause of death of mice that lack all lymphatic vessels due to loss of the secreted lymphangiogenic factor CCBE1 or signaling by the lymphatic endothelial receptor VEGFR3. We find that loss of lymphatic function has no major cardiovascular effects before birth, but that lymphatic-deficient animals die immediately after birth due to respiratory failure. Neonatal respiratory failure in lymphatic-deficient animals is not due to impaired gas exchange, compressive pleural effusions, or an unexpected role for lymphatic vessels in the molecular or cellular development of the lung. Instead, lymphatic function is required before birth in the late gestation lung to increase lung compliance and alter lung mechanics in preparation for inflation at birth. These studies reveal new insights into the function of the lymphatic system during lung development that explain respiratory failure in infants with congenital pulmonary lymphangiectasia, and identify an organ-specific, mechanical role for lymphatic vessels that may contribute to RDS in premature infants.

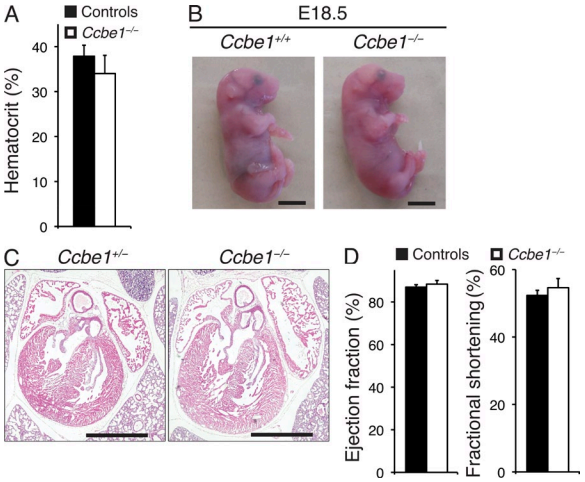

Figure 1. Non-anemic *Ccbe1*$^{-/-}$ embryos survive to late gestation with normal cardiovascular function. (A) E17–18 *Ccbe1*$^{-/-}$ embryos that did not appear pale were selected for studies of lung function. The hematocrits of non-pale *Ccbe1*$^{-/-}$ embryos were not reduced compared with littermate controls. Quantitative data are represented as mean and SEM from 8 control and 5 *Ccbe1*$^{-/-}$ embryos from 3 independent litters (P = 0.40). (B) Gross appearance of *Ccbe1*$^{-/-}$ and control littermate embryos at E18.5. Representative images are shown from 81 control and 20 *Ccbe1*$^{-/-}$ E18.5 embryos examined from 15 litters. Bars, 5 mm. (C) Cardiac size and structure of *Ccbe1*$^{-/-}$ and control littermate embryos are shown at E18.5 by H-E staining. Images are representative of 5 control and 5 *Ccbe1*$^{-/-}$ embryos examined from 3 independent litters. Bars, 1,000 µm. (D) Cardiac ejection fraction and fractional shortening of E18.5 *Ccbe1*$^{-/-}$ and littermate control embryos determined by transuterine ultrasound. Quantitative data for ejection fraction and fractional shortening are represented as mean and SEM from 7 control and 4 *Ccbe1*$^{-/-}$ embryos examined from 3 independent litters (P = 0.2 and P = 0.14 for ejection fraction and fractional shortening, respectively).

RESULTS

CCBE1-deficient animals lacking lymphatic vessels do not die in utero

Mutant mice that lack all lymphatics (e.g., those lacking the lymphatic endothelial transcription factor PROX1 [Wigle and Oliver, 1999], the lymphangiogenic factors VEGFC [Karkkainen et al., 2004] or CCBE1 [Zou et al., 2013], or the lymphatic endothelial growth factor receptor VEGFR3 [Karkkainen et al., 2001; Zhang et al., 2010]) do not survive past birth, but when and why animals lacking lymphatic vessels die has not been established. Analysis of midgestation *Ccbe1*$^{-/-}$ embryos revealed normal blood vascular development, a complete lack of lymphatic vessels, and one third of deficient animals exhibited midgestation embryonic anemia on a mixed 129SV;C57BL/6 background (Zou et al., 2013). No live *Ccbe1*$^{-/-}$ neonates were recovered at postnatal day 0.5 (P0.5), but two thirds of *Ccbe1*$^{-/-}$ embryos were not pale and had normal hematocrits at embryonic day 17.5–18.5 (E17.5–18.5; Fig. 1 A). Like embryos lacking VEGFC or VEGFR3 signaling (Karkkainen et al., 2001, 2004; Zhang et al., 2010), E14.5 *Ccbe1*$^{-/-}$ embryos exhibited marked midgestation cutaneous edema (Zou et al., 2013), but this improved in late gestation and by E18.5 *Ccbe1*$^{-/-}$ embryos were frequently indistinguishable from control littermates (Fig. 1 B). It has been thought that lymphatic-deficient animals die due to loss of intravascular fluid which leads to cardiovascular collapse and death, but histological analysis and trans-uterine ultrasound revealed normal heart structure and function in E18.5–19.5 CCBE1-deficient embryos (Fig. 1, C and D). These findings reveal that *Ccbe1*$^{-/-}$ embryos do not die prenatally due to cardiovascular causes.

CCBE1-deficient and Vegfr3$^{kd/kd}$ neonates are cyanotic and die of respiratory failure

To determine if CCBE1-deficient animals die around the time of birth, heterozygous matings were performed and offspring retrieved immediately after natural birth. All wild-type and *Ccbe1*$^{+/-}$ pups achieved a pink color consistent with normal tissue oxygenation within 5–20 min and were viable for >60 min after delivery (Fig. 2 A). In contrast, almost all *Ccbe1*$^{-/-}$ pups appeared severely cyanotic and died within 3 h (Fig. 2 A). An identical phenotype was observed when *Ccbe1*$^{-/-}$ pups were retrieved by Caesarean (C) section at E19.5 (Fig. 2 B, n = 12/13; P < 0.0001 compared with control), whereas all control littermates achieved a pink color and

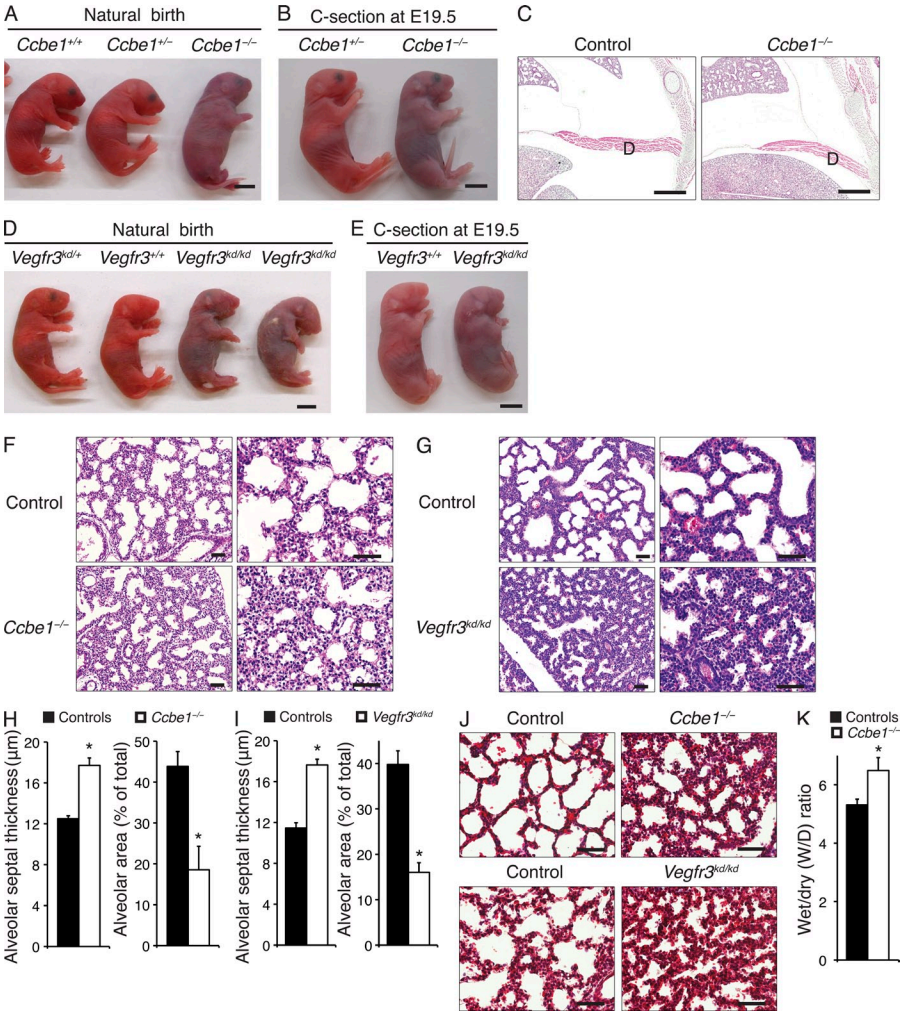

Figure 2. Animals lacking lymphatic vessels exhibit cyanosis and respiratory failure immediately after birth. (A) Cyanotic state of *Ccbe1*$^{-/-}$ neonates after natural birth. Representative littermates are shown. Bar, 5 mm. (B) Cyanotic state of *Ccbe1*$^{-/-}$ neonates after C-section at E19.5. Bar, 5 mm. These animals are also shown in Video 1. Representative neonates are shown from 47 littermate control and 13 *Ccbe1*$^{-/-}$ animals examined from 8 independent litters. (C) H-E staining of the diaphragms of *Ccbe1*$^{-/-}$ and control littermate embryos. Frontal sections of the intact chest of the indicated E18.5 embryos were stained with H-E. Bars, 500 µm. D indicates diaphragm. The images are representative of 3 control and 3 *Ccbe1*$^{-/-}$ embryos examined at E18.5 from 3 independent litters. (D) Cyanotic state of *Vegfr3*$^{kd/kd}$ neonates after natural birth compared with control littermates. Bar, 5 mm. (E) Cyanotic state of *Vegfr3*$^{kd/kd}$ neonates after C-section at E19.5 compared with control littermates. Bar, 5 mm. These animals are also shown in Video 2. Representative images are shown from 35 littermate control and 13 *Vegfr3*$^{kd/kd}$ neonates examined from 6 independent litters. Images in A, B, D, and E were obtained 30 min after birth or C-section. (F and G) H-E staining of lung sections to show alveolar septae and alveolar air spaces in *Ccbe1*$^{-/-}$ and cyanotic *Vegfr3*$^{kd/kd}$ neonates compared with control littermates 60 min after birth. Bars, 50 µm. Representative images are shown from 5–6 control and 4–5 lymphatic deficient neonates examined from 3–4 independent litters in each group. (H and I) Measurement of alveolar septal thickness and area in *Ccbe1*$^{-/-}$, cyanotic *Vegfr3*$^{kd/kd}$ neonates, and littermate controls. Quantitative data are represented as mean and SEM for septal thickness and alveolar area. n = 5–6 control and 4–5 lymphatic-deficient neonates per genotype from 3–4 litters in each group (*Ccbe1*$^{-/-}$: $P < 0.001$ and $P < 0.01$ for septal thickness and alveolar area, respectively; *Vegfr3*$^{kd/kd}$: $P < 0.0001$ and $P < 0.001$ for septal thickness and alveolar area, respectively). (J) Trichrome staining of alveolar septae and alveolar area in *Ccbe1*$^{-/-}$ and cyanotic *Vegfr3*$^{kd/kd}$ neonatal lungs compared with control littermates 60 min after birth. Bars, 50 µm. Representative images are shown from 3 control and 3 lymphatic deficient neonates from 3 independent litters examined in each group. (K) *Ccbe1*$^{-/-}$ and control neonate lung wet/dry (W/D) ratios of lung weight. Quantitative data are represented as mean and SEM from 10 control and 3 *Ccbe1*$^{-/-}$ neonates from 2 independent litters ($P = 0.02$). Asterisks indicate $P < 0.05$ compared with control.

survived (n = 47). *Ccbe1*$^{-/-}$ pups had normal diaphragms and exhibited gasping and costal retractions, indicative of normal neuromuscular function and respiratory drive (Fig. 2 C and Video 1). Thus, CCBE1-deficient mice lacking lymphatics exhibit respiratory failure immediately after birth, and die soon thereafter.

Respiratory failure in CCBE1-deficient neonates could reflect a requirement for lymphatic function for neonatal respiration, or an unexpected role for CCBE1 in lung development. Because the mechanism of action of secreted CCBE1 is unknown, to further define the role of lymphatic function in neonatal respiration we next examined *Vegfr3*$^{kd/kd}$ mice that lack lymphatic vessels due to a point mutation in the kinase domain of VEGFR3. VEGFR3 function is required cell autonomously for lymphatic endothelial and vessel growth (Mäkinen et al., 2001), and its expression is entirely restricted to lymphatic endothelial cells in the developing lung (Kaipainen et al., 1995; Janér et al., 2006; Kulkarni et al., 2011). The *Vegfr3*^{kd} allele encodes a dominant-negative protein that confers postnatal lethality in heterozygous animals that is ameliorated on specific permissive genetic backgrounds (i.e., C3H or NMRI; Karkkainen et al., 2001; Zhang et al., 2010). Observation of natural births and C-section at E19.5 revealed cyanosis and respiratory failure in *Vegfr3*$^{kd/kd}$ but not wild-type or *Vegfr3*$^{kd/+}$ neonates which was identical to that observed in *Ccbe1*$^{-/-}$ neonates (n = 8/13 in the C-section group, discussed further below; Fig. 2, D and E; and Video 2).

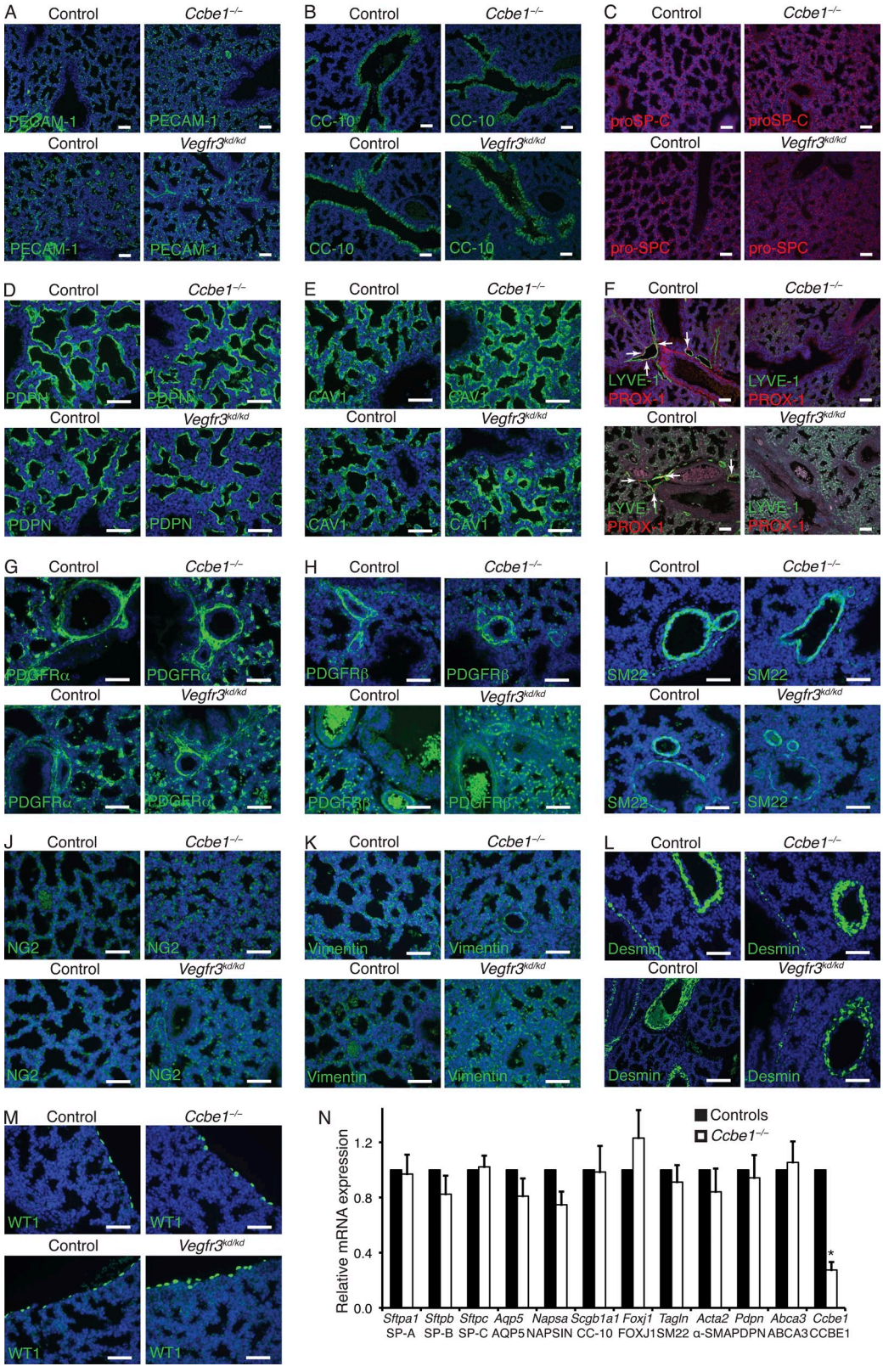

Figure 3. Loss of CCBE1 or VEGFR3 signaling does not affect the development of lung cell types other than lymphatic vessels. (A–M) E18.5 *Ccbe1*$^{-/-}$, *Vegfr3*$^{kd/kd}$, and control littermate embryonic lungs were stained for markers of lung endothelial cells (PECAM), lung Clara cells (CC-10), alveolar Type II cells (pro-surfactant protein C [SPC]), Type I cells (PODOPLANIN [PDPN] and CAVEOLIN1 [CAV1]), lymphatic endothelial cells (PROX1 and LYVE1), mesenchyme (PDGFRα), vascular smooth muscle cells and pericytes (PDGFRβ, SM22 and NG2), blood vessels (vimentin and desmin), and mesothelium

Loss of lymphatic function results in pulmonary edema but does not alter molecular or cellular lung development

H-E staining of lung tissue sections from both *Ccbe1*$^{-/-}$ and cyanotic *Vegfr3*$^{kd/kd}$ neonates revealed normal lung structure, but alveolar interstitial thickness was significantly increased and alveolar area significantly reduced compared with control littermates 60 min after birth (Fig. 2, F–I). These changes were also easily detected using trichrome staining of control and mutant neonatal lungs (Fig. 2 J). Measurement of the lung wet/dry (W/D) ratio 60 min after C-section revealed a significantly higher fluid content in *Ccbe1*$^{-/-}$ lungs (Fig. 2 K), consistent with pulmonary edema. In contrast, immunostaining revealed a normal PECAM^{+} blood vascular endothelial network, normal numbers of CC10^{+} Clara cells and pro-SPC^{+} Type II pneumocytes, and a total lack of PROX1^{+};LYVE1^{+} lymphatic vessels in neonatal *Ccbe1*$^{-/-}$ and *Vegfr3*$^{kd/kd}$ lungs (Fig. 3, A–C). Staining for the Type I cells markers podoplanin and caveolin1 was similar in control, *Ccbe1*$^{-/-}$, and *Vegfr3*$^{kd/kd}$ lungs (Fig. 3, D and E). Finally, extensive immunostaining and qPCR analysis of lung developmental markers revealed normal levels of mesenchymal markers (PDGFRα), vascular smooth muscle cells and pericytes (PDGFRβ, SM22, and NG2), blood vessel markers (vimentin [Schnitzer et al., 1981] and desmin [Morikawa et al., 2002]), and mesothelial cells (Fig. 3, F–N). These studies reveal that neonatal respiratory failure is due to loss of lymphatic fluid drainage rather than loss of the specific molecular action of CCBE1 or VEGFR3, and that loss of lymphatic function does not disturb molecular or cellular maturation of the lung.

Mice lacking lymphatic function are unable to inflate their lungs after birth

Why do mice lacking lymphatic vessels exhibit cyanosis and respiratory failure after birth? The preservation of lung development and cardiovascular function supported a defect in pulmonary physiology, and the thickened alveolar walls and elevated W/D ratio suggested that cyanosis might result from reduced oxygen diffusion. To determine if cyanosis was due to reduced oxygen diffusion, *Ccbe1*$^{-/-}$ neonates were exposed to 100% oxygen for 30 min. 100% oxygen failed to improve cyanosis (Fig. 4 A, $n = 3$), indicating the passage of blood through the lung without gas exchange. The physiological basis for this shunt was revealed by comparison of rare non-cyanotic *Ccbe1*$^{-/-}$ neonates (1/13) and more frequent non-cyanotic *Vegfr3*$^{kd/kd}$ neonates (5/13) with their cyanotic littermates. Lungs from all non-cyanotic *Ccbe1*$^{-/-}$ and *Vegfr3*$^{kd/kd}$ neonates floated when placed in saline, whereas those from all cyanotic *Vegfr3*$^{kd/kd}$ or *Ccbe1*$^{-/-}$ neonates sank (Figs. 4, B and C; $n = 9$, $P < 0.003$), indicating that cyanosis resulted from a failure of lung inflation. Histological examination of non-cyanotic *Vegfr3*$^{kd/kd}$ neonates revealed small pockets of normal-appearing lung with thin interstitia and large alveoli, suggesting that partial inflation of the lung was sufficient to oxygenate the neonate and allow the excised lung to float (Fig. 4 D). These findings identify failure of lung inflation as the cause of respiratory failure in mice without lymphatic vessels. The higher frequency of partial lung inflation among *Vegfr3*$^{kd/kd}$ neonates compared with *Ccbe1*$^{-/-}$ neonates most likely reflects effects of the specific genetic backgrounds (C3H and NMRI) that ameliorate the effects of dominant-negative VEGFR3 kinase-dead receptor expression, and permit the survival of *Vegfr3*$^{kd/+}$ animals that are also highly deficient in lymphatic function (Martel et al., 2013).

Failure of lung inflation is not due to surfactant deficiency or compressive pleural effusions

Initial inflation of the neonatal lung requires much greater force than subsequent inflations, even those occurring only minutes later (Milner and Sauders, 1977; Guyton and Hall, 2000). Thus, a primary obstacle to neonatal lung inflation is the mechanical force needed to open the embryonic lung and allow the first entry of air into alveoli. The critical known regulator of this mechanical force is surfactant, a protein-phospholipid mix that increases pulmonary compliance through effects on alveolar surface tension and is required for lung inflation (Nogee et al., 1994; Clark et al., 1997). E19.5 *Ccbe1*$^{-/-}$ and *Vegfr3*$^{kd/kd}$ lungs contained normal levels of pro-SPC (Fig. 3 C), normal amounts of glycogen (a surfactant precursor that accumulates with a block in surfactant production; Bourbon et al., 1982; Compernolle et al., 2002; Fig. 5, A and B), and normal amounts of total lung phospholipid (Fig. 5 C). In addition, transmission electron microscopy of E19.5 *Ccbe1*$^{-/-}$ embryo lungs revealed a normal number and morphology of both Type I and Type II pneumocytes, including the presence of typical lamellar bodies, and abundant extracellular, alveolar surfactant (Fig. 5, D and E; representative of three *Ccbe1*$^{-/-}$ and littermate control lungs studied). These studies eliminate loss of surfactant as the basis for failure of lung inflation in neonates lacking lymphatic function.

A second means by which loss of lymphatic function might prevent lung inflation is through external compression of the lung by pleural effusions that might accumulate in the absence of lymphatic drainage. To address this possibility, we histologically examined the intact chests of *Vegfr3*$^{kd/kd}$ and *Ccbe1*$^{-/-}$ neonates. Cyanotic lymphatic-deficient neonates often had minimal pleural effusions (e.g., Fig. 5 F and Fig. 2 C), whereas

(Wilms Tumor 1 [WT1]). Bars, 50 µm. Representative images are shown from 3 control and 3 lymphatic-deficient embryos examined from 3 independent litters in each group. Arrows indicate PROX1^{+} nuclei surrounded by LYVE1^{+} cell membrane in lymphatic endothelial cells (F). (N) qPCR was used to measure relative mRNA expression levels of the indicated lung cell marker genes in littermate control and *Ccbe1*$^{-/-}$ neonatal lungs after C-section at E18.5. Quantitative data are represented as mean and SEM from 5–7 control and 4–6 *Ccbe1*$^{-/-}$ E18.5 embryos examined from 2 independent litters in each group. Asterisk indicates $P < 0.05$ compared with control.

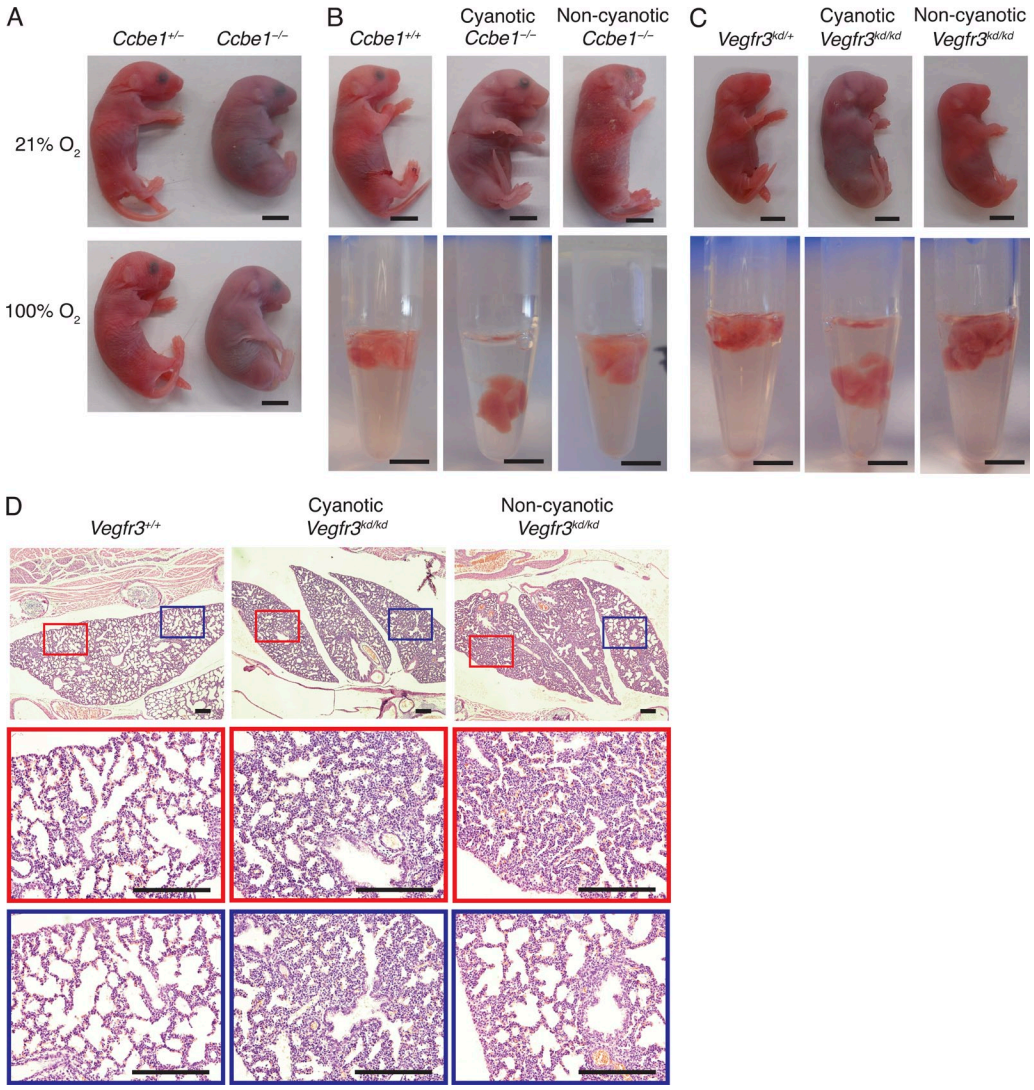

Figure 4. Neonatal respiratory failure in mice lacking lymphatics results from failure of lung inflation. (A) Exposure of *Ccbe1*$^{-/-}$ and littermate control neonates to 100% oxygen (O_2) for 30 min. Bars, 5 mm. Images are representative of 4 control and 3 *Ccbe1*$^{-/-}$ neonates from 1 litter. (B and C) Flotation of cyanotic *Ccbe1*$^{-/-}$ and *Vegfr3*$^{kd/kd}$ neonate lungs in saline compared with control littermates and non-cyanotic *Ccbe1*$^{-/-}$ or *Vegfr3*$^{kd/kd}$ neonatal lungs. Bars, 5 mm. Images are representative of 24 control and 9 lymphatic-deficient neonates examined from 5 independent experiments. (D) H-E–stained sections of lung from cyanotic and non-cyanotic neonates. Bars, 200 µm. Representative images are shown from 6 control, 5 cyanotic, and 3 non-cyanotic *Vegfr3*$^{kd/kd}$ neonates examined from 4 independent litters in each group.

lymphatic-deficient neonates with the largest pleural effusions were frequently not cyanotic due to successful inflation of a part of the lung (Fig. 5 F). Thus, lung inflation in neonates lacking lymphatic function did not correlate with either the presence or size of an associated pleural effusion. To genetically test the requirement for pleural lymphatic function in neonatal respiration, we generated WT1-Cre;*Ccbe1*$^{flox/flox}$ animals in which CCBE1 is deleted from the mesothelium that forms the pleura. WT1-Cre;*Ccbe1*$^{flox/flox}$ animals lacked all pleural lymphatic vessels (Fig. 5 G) but did not exhibit neonatal respiratory failure (Fig. 5 H). These observations suggest that failure of lung inflation reflects a lung-intrinsic, mechanical requirement for lymphatic function distinct from that of surfactant.

Pulmonary lymphatic function is present before birth

Previous studies of lymphatic function around the time of birth have used catheter-based flow measurements to demonstrate that lymphatic drainage from the lung does not rise significantly during or immediately after birth in lambs (Bland et al., 1982). These studies suggested that lymphatic function might be required prenatally, and not merely around the time of birth, for neonatal lung inflation. Lymphatic endothelial cells are present in the lung as early as E12.5 and lymphatic vessels with visible lumens can be seen as early as E14.5 (Kulkarni et al., 2011), but whether pulmonary lymphatics function before birth is not known. To measure lymphatic function in the prenatal lung, we injected rhodamine-dextran through the uterine and chest walls into the lungs of live *Prox1*^{GFP} transgenic

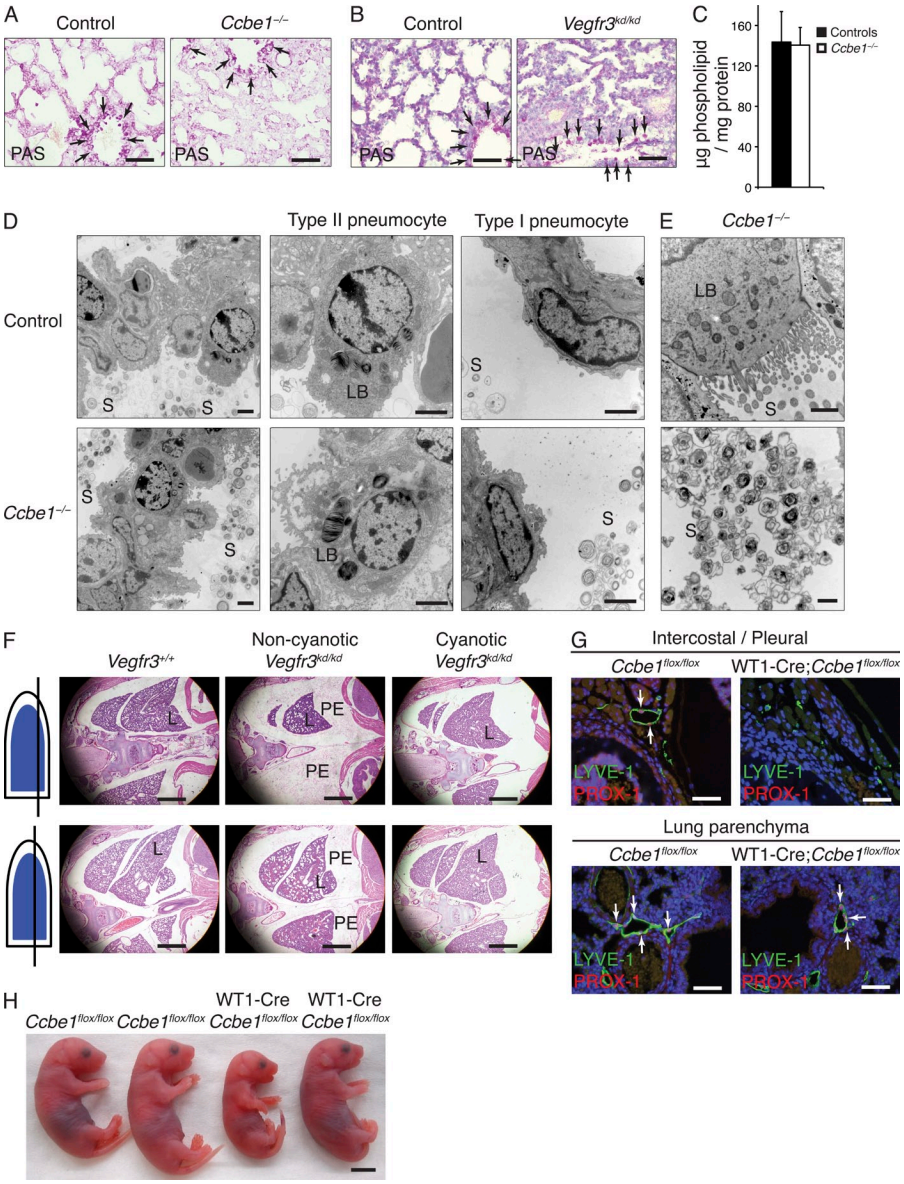

Figure 5. Lack of lung inflation in neonates lacking lymphatics is not due to surfactant deficiency or the effect of large pleural effusions. (A and B) Periodic acid-Schiff (PAS) staining for levels of the surfactant precursor glycogen in the lungs of *Ccbe1*$^{-/-}$, *Vegfr3*$^{kd/kd}$, and control littermate neonates. Bars, 50 µm. Representative images are shown from 5–6 littermate control and 4–5 lymphatic-deficient neonates per genotype examined from 3–4 litters in each group. Arrows indicate glycogen-rich cells in the large airways. (C) Phospholipid content of *Ccbe1*$^{-/-}$ and littermate control neonatal lungs. Quantitative data are represented as mean and SEM from 3 control and 5 *Ccbe1*$^{-/-}$ animals examined from 2 independent litters (P = 0.93). (D) Transmission electron microscopy of the lungs of *Ccbe1*$^{-/-}$ neonates reveals surfactant (S) in pulmonary alveoli (left), the presence of lamellar bodies (LB) in Type II pneumocytes (middle), and Type I alveolar pneumocytes (right). Bars, 2 µm. Images are representative of 3 animals studied for each genotype from 2 independent litters. (E) Representative images of active surfactant secretion and abundant alveolar surfactant are shown in *Ccbe1*$^{-/-}$ lungs using electron microscopy. Bars, 1 µm. (F) H-E–stained sections of the intact chest of *Vegfr3*$^{+/+}$, non-cyanotic *Vegfr3*$^{kd/kd}$, and cyanotic *Vegfr3*$^{kd/kd}$ neonates are shown. The schematic on the left indicates the approximate plane of frontal section for each set of images. The location of lung (L) and pleural effusion (PE) are indicated. Note the presence of a very large effusion in this non-cyanotic *Vegfr3*$^{kd/kd}$ neonate compared with that of a cyanotic *Vegfr3*$^{kd/kd}$ littermate. Bars, 1,000 µm. (G) LYVE1-PROX1 staining for intercostal (top) and lung parenchymal (bottom) lymphatic vessels in WT1-Cre;*Ccbe1*$^{flox/flox}$ and littermate control animals. Arrows indicate PROX1^{+} nuclei surrounded by LYVE1^{+} cell membrane in lymphatic endothelial cells. Bars, 50 µm. (H) Non-cyanotic WT1-Cre;*Ccbe1*$^{flox/flox}$ animals after C-section at E19.5. Representative images are shown examined from 10 littermate control and 3 WT1-Cre;*Ccbe1*$^{flox/flox}$ embryos from 2 independent litters (G and H). Bar, 5 mm.

embryos at E18.5. Selective uptake and passage of rhodamine-dextran in GFP^{+} lymphatic vessels was readily detected (Fig. 6 A), demonstrating active lymphatic drainage of the late gestation mouse lung. Similar studies revealed active lymphatic function with luminal rhodamine-dextran in GFP^{+} lymphatics at E17.5 (Fig. 6, B and C). To further investigate the impact of prenatal pulmonary lymphatic function, we next examined the lungs of late gestation *Ccbe1*$^{-/-}$ and *Vegfr3*$^{kd/kd}$ embryos that were harvested after immersion of the gravid uterus in ice-cold saline for 45 min, an approach which preserves the late gestation chest and lung as they exist in utero before any air inflation. The E16.5 mouse lung lacks well-formed alveoli, and *Ccbe1*$^{-/-}$ and *Vegfr3*$^{kd/kd}$ lungs were indistinguishable from those of control littermates at this time point (Fig. 6, B and C). At E17.5 alveoli are present, and while some *Ccbe1*$^{-/-}$ and *Vegfr3*$^{kd/kd}$ lungs did not differ markedly from those of control littermates (e.g., Fig. 6 D), others displayed thickened septae and smaller alveolar area (e.g., Fig. 6 E). By E18.5, the alveoli of all *Ccbe1*$^{-/-}$ and *Vegfr3*$^{kd/kd}$ embryonic lungs appeared smaller than those of control littermates, the alveolar septae were significantly thicker, and the alveolar was significantly reduced (Fig. 6, D–G). Consistent with molecular findings supporting normal growth and maturation of lung cell types in *Ccbe1*$^{-/-}$ and *Vegfr3*$^{kd/kd}$ embryos, the DNA content and dry weights of E18.5 *Ccbe1*$^{-/-}$ lungs were similar to those of control littermates (Figs. 6, H and I). These findings indicate that lymphatic vessels function

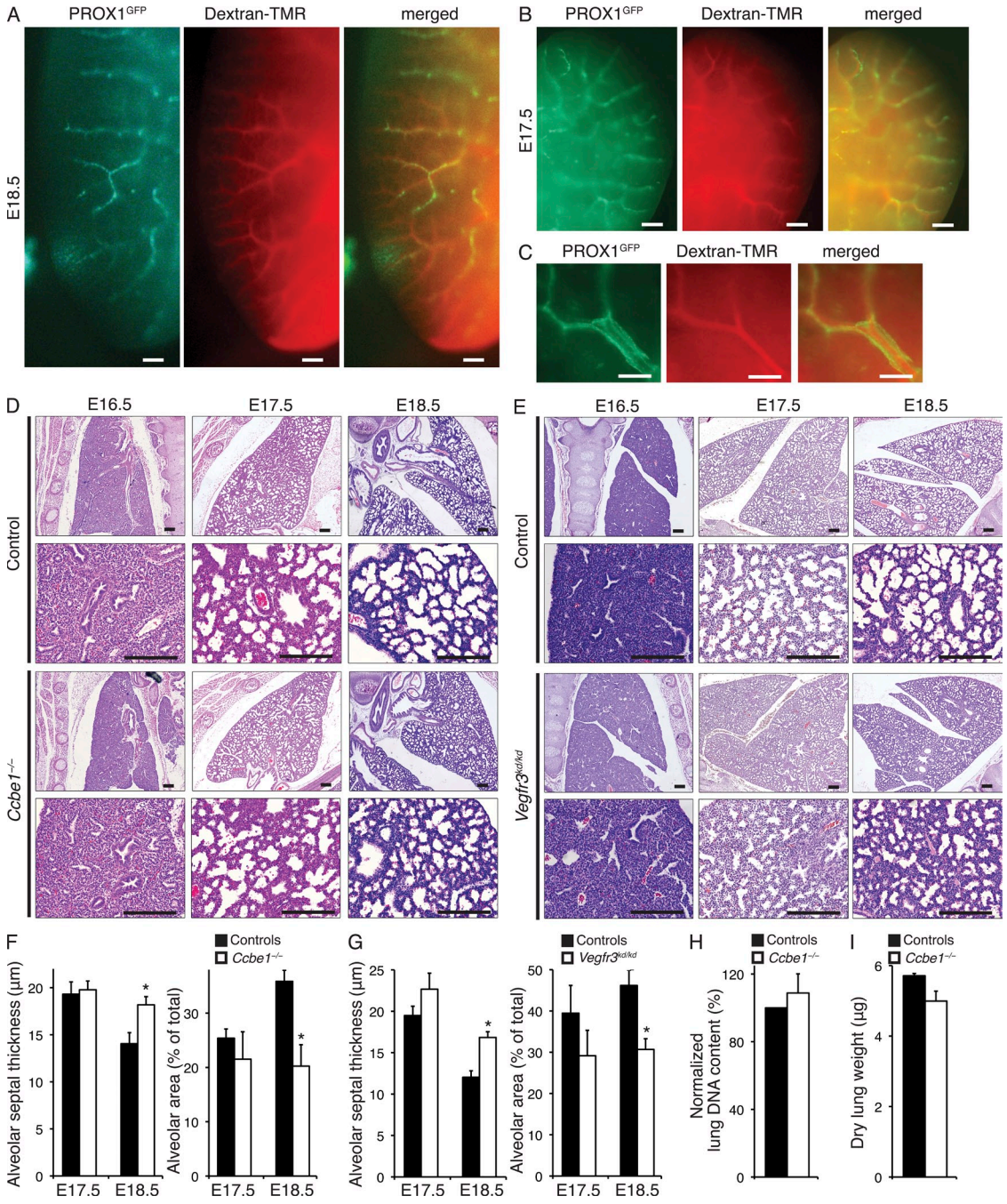

Figure 6. The lung lymphatic vascular network is functional during late gestation. (A) Rhodamine-labeled dextran (dextran-TMR) injected into the lungs of live E18.5 *Prox1*^{GFP} transgenic embryos is selectively taken up by GFP$^+$ lymphatic vessels. Bars, 250 µm. (B and C) Rhodamine-labeled dextran (dextran-TMR) injected into the lungs of live E17.5 *Prox1*^{GFP} transgenic embryos is detected in the lumen of GFP$^+$ lymphatic vessels (C). Bars, 250 µm. Representative images in A–C are shown from 6 embryos from 4 litters. (D and E) H-E staining of *Ccbe1*$^{-/-}$, *Vegfr3*$^{kd/kd}$, and littermate control embryonic lungs harvested after uterine immersion in ice-cold saline to preserve their in utero state at E16.5, E17.5, and E18.5. Bars, 200 µm. Representative images are shown from 3–7 control and 3–7 lymphatic-deficient embryos per time point examined from 2–4 independent litters. (F) Measurement of alveolar septal thickness and alveolar area in *Ccbe1*$^{-/-}$ and littermate control lungs at E17.5 and E18.5. Quantitative data represent mean and SEM from 3–7 control and 3–7 *Ccbe1*$^{-/-}$ embryos per time point from 2–4 independent litters (P = 0.015 and P = 0.005 for septal thickness and alveolar area at E18.5, respectively). (G) Measurement of alveolar septal thickness and alveolar area in *Vegfr3*$^{kd/kd}$ and littermate control lungs at E17.5 and E18.5. Quantitative data represent mean and SEM from 3 control and 3 *Vegfr3*$^{kd/kd}$ embryos per time point examined from 3 independent litters (P = 0.02 and P = 0.05 for septal thickness and alveolar area at E18.5, respectively). (H) DNA content in E18.5 *Ccbe1*$^{-/-}$ and littermate control lungs. Quantitative data are represented as mean and SEM from 13 control and 8 *Ccbe1*$^{-/-}$ embryos examined from 3 independent litters (P = 0.58). (I) Dry weight of E18.5-19.5 *Ccbe1*$^{-/-}$ and littermate control lungs. Quantitative data are represented as mean and SEM examined from 21 control and 7 *Ccbe1*$^{-/-}$ embryos from 5 independent litters (P = 0.29). Asterisks indicate P < 0.05 compared with control.

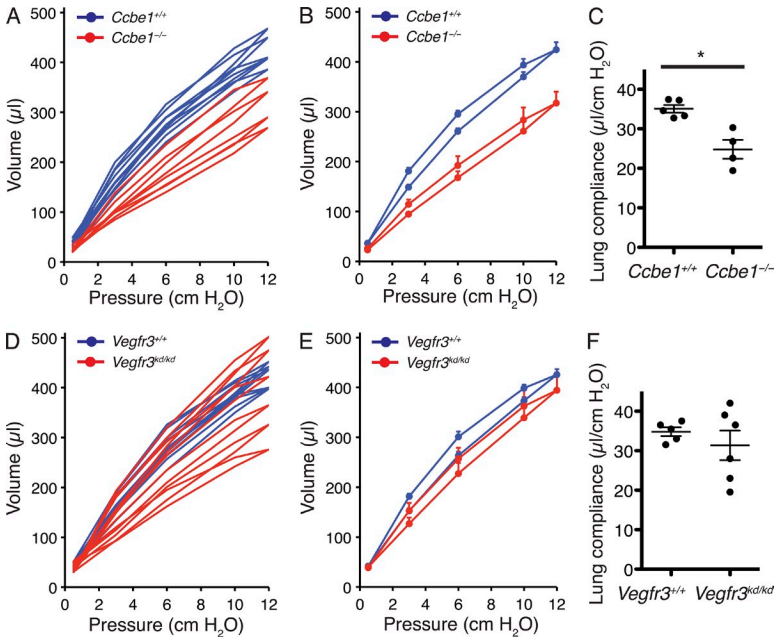

Figure 7. Lymphatic function is required to increase lung compliance in late gestation. (A) Individual pressure-volume (P-V) curves for 5 *Ccbe1*$^{+/+}$ and 4 *Ccbe1*$^{-/-}$ lungs examined from 3 independent litters at E18.5 are shown. (B) P-V curves from the samples in A are represented as mean and SEM. (C) The calculated compliance of *Ccbe1*$^{-/-}$ lungs compared with that of wild-type littermates at E18.5. Error bars represent mean and SEM from 5 *Ccbe1*$^{+/+}$ and 4 *Ccbe1*$^{-/-}$ lungs examined from 3 independent litters ($P = 0.003$). (D) Individual pressure-volume (P-V) curves for 5 *Vegfr3*$^{+/+}$ and 6 *Vegfr3*$^{kd/kd}$ lungs examined from 2 independent litters at E18.5 are shown. (E) P-V curves from the samples in D are represented as mean and SEM. (F) The calculated compliance of *Vegfr3*$^{kd/kd}$ lungs compared with that of wild-type littermates at E18.5. Error bars represent mean and SEM from 5 *Vegfr3*$^{+/+}$ and 6 *Vegfr3*$^{kd/kd}$ lungs examined from 2 independent litters ($P > 0.05$). Asterisk indicates $P < 0.05$ compared with control.

before birth, and that changes in lung architecture associated with loss of prenatal lymphatic function are not secondary to reduced growth or increased matrix production.

Lymphatic function is required to increase lung compliance in late gestation

The prenatal lymphangiograms and histological changes observed in lymphatic-deficient lungs suggested that lymphatic function might affect lung structure through changes in the physical/mechanical characteristics of the developing lung. The lung expands late in gestation, an event attributed to active fetal breathing movements (Patrick and Challis, 1980; Kobayashi et al., 2001). We therefore hypothesized that loss of lymphatic function may reduce intrinsic lung compliance, resulting in reduced lung expansion in utero and failure of lung inflation after birth. To test this hypothesis, we measured the total lung compliance of E18.5 lungs that were harvested from embryos sacrificed by uterine immersion in ice-cold saline. Pressure-volume curves revealed a significant reduction in the compliance of prenatal *Ccbe1*$^{-/-}$ lungs compared with those of prenatal *Ccbe1*$^{+/+}$ control littermates (Fig. 7, A–C, $n = 4$, $P < 0.003$). A similar reduction in prenatal compliance was observed in some but not all E18.5 *Vegfr3*$^{kd/kd}$ lungs (Fig. 7, D–F, $n = 6$, $P > 0.05$), consistent with the greater variability in neonatal cyanosis observed in *Vegfr3*$^{kd/kd}$ animals compared with *Ccbe1*$^{-/-}$ animals (12/13 cyanotic *Ccbe1*$^{-/-}$ neonates vs. 8/13 cyanotic *Vegfr3*$^{kd/kd}$ neonates). Collectively, these studies reveal that lymphatic function increases lung compliance before birth, and that this process contributes to successful lung inflation after birth.

DISCUSSION

Of the many physiological challenges that face neonatal mammals, successful respiration is the most dramatic and one that must be met immediately for survival. Successful neonatal respiration relies upon a developmental program that prepares the lung for air inflation while it forms in a fluid environment. In addition to the molecular and cellular events required to create lung airways and alveoli, a critical part of this developmental preparation is the acquisition of mechanical properties that allow the fluid-filled lung to inflate with air after birth. The importance of such mechanical preparation is revealed by the failure of lung inflation and neonatal respiration in both mice and humans that lack surfactant (Nogee et al., 1994; Clark et al., 1997), a product of alveolar Type II cells which increases lung compliance by reducing alveolar surface tension.

Our studies identify lymphatic function as a second mechanism by which the developing mammalian lung is mechanically prepared for inflation at birth. Analysis of late gestation and neonatal lungs from mice lacking lymphatic vessels revealed no changes in the molecular or cellular development of the lung, but increased W/D ratios indicated the presence of pulmonary edema. These findings suggest that interstitial pulmonary edema is responsible for the reduced lung compliance before birth, and for the failure of lung inflation at the time of birth observed in the absence of lymphatic function. Precisely how pulmonary edema reduces compliance is not yet clear, but it seems likely that edema changes the intrinsic elastic properties of the lung tissue without altering its cellular or molecular composition. This model is consistent with mechanical studies of adult humans and dogs performed more than 50 years ago that revealed reduced lung compliance with the onset of acute pulmonary edema (Sharp et al., 1958; Haddy and Haddy, 1964). The effects of reduced compliance in the mature lung were not as drastic as those we observe in the prenatal and neonatal lung, but these studies demonstrate that edema alters the intrinsic compliance of an otherwise normal

lung. Our findings are also consistent with a previous study that reported reduced postnatal survival of mice in which a dominant-negative VEGFR3 ectodomain inhibited lymphatic growth specifically in the lung (Kulkarni et al., 2011). However, because these animals retained some lymphatic function and were not cyanotic at birth, the prenatal role of lymphatic vessels in the lung was not revealed by these studies.

Why do lymphatics play such an important mechanical role in the developing and neonatal lung? There are several molecular and physiological explanations for this observation. The lung develops with abundant airway luminal fluid that is required for normal organ growth (Moessinger et al., 1990). In late gestation and immediately after birth this fluid is actively transported from the airway into the interstitium by the epithelial sodium channel ENaC in a process that is required for neonatal respiration (Hummler et al., 1996). Thus, the late gestation and neonatal lung acquires excess interstitial fluid by a mechanism of active transport that is not active in the mature animal. In addition, interstitial fluid is removed from the lung through Starling forces in the lung blood vascular capillary network much more efficiently after birth due to large increase in pulmonary blood flow that accompanies closure of the ductus arteriosus. Finally, initial inflation of the lung requires much greater negative inspiratory pressure than does inflation at later time points after birth and in mature animals (Milner and Sauders, 1977; Guyton and Hall, 2000). Thus, any reduction in compliance due to interstitial edema is likely to have a smaller effect in mature animals compared with a neonate attempting to take its first breath. This unique set of molecular and physiological conditions is likely to explain why lymphatic drainage of interstitial fluid in the late gestation lung is essential for lung inflation.

An important clinical question raised by these mouse genetic studies is whether and to what extent loss of lymphatic function might affect neonatal respiration in human infants. Human infants with congenital pulmonary lymphangiectasia (CPL), a rare disorder associated with primary pulmonary lymphatic defects, experience cyanosis and death immediately after birth that is identical to the phenotype we observe in *Ccbe1*$^{-/-}$ and *Vegfr3*$^{kd/kd}$ neonatal mice (Laurence, 1955; Noonan et al., 1970). CPL has also been reported in association with Hennekam syndrome (Bellini et al., 2003), a primary human lymphatic disorder which may result from loss of CCBE1 (Alders et al., 2009), indicating that our findings in mice are likely to apply to human neonatal lung inflation.

RDS in premature infants is attributed primarily to a lack of surfactant that is not produced until late gestation. Our histological studies do not reveal significant differences between control and lymphatic-deficient embryo lungs until E18.5, suggesting that, like surfactant, lymphatic function may be most active in the period immediately preceding birth. Thus, the mechanical role of lymphatics in the developing lung is likely to overlap both temporally and functionally with that of pulmonary surfactant, and inadequate lymphatic function may contribute significantly to the RDS experienced by premature infants. Future studies that specifically address the role of lymphatic function in premature infants may lead to new approaches to the prevention and management of RDS that focus on reducing pulmonary edema.

MATERIALS AND METHODS

Animals. The *Ccbe1*^{LacZ}-null allele was generated by our laboratory as described previously (referred as *Ccbe1*$^{-}$; Zou et al., 2013) and maintained on a 129SV:C57BL/6 mixed background. The offspring of heterozygous matings was genotyped by allele-specific PCR using 5′-TGGGAGTTGAATCCCTGATGGTCT-3′ forward and 5′-AGGCCATACAAGTGTTGGGCATTG-3′ reverse null allele-specific, and 5′-CAGAGCAAAGGGACAACAGGTG-3′ forward and 5′-TAAACACGGCAGCAGCAACC-3′ reverse wild-type allele-specific primers. The *Ccbe1*^{flox} allele was generated by our laboratory as described previously (Zou et al., 2013). WT1-Cre animals were obtained from The Jackson Laboratory (JAX #010911). Mice carrying the kinase-dead *Vegfr3* allele (aka *Chy* mice; MRC Harwell) were maintained on a NMRI/C3H mixed background (Karkkainen et al., 2001). The *Vegfr3*^{kd} point mutant allele was genotyped using 5′-CTGGCTGAGTCCCTAACTCG-3′ forward and 5′-CGGGGTCTTTGTAGATGTCC-3′ reverse primers, followed by a restriction enzyme digestion with BglII as previously described (Zhang et al., 2010). *Prox1*^{GFP} BAC transgenic mice were obtained from the Mutant Mouse Regional Resource Centers (MMRRC). All animal experiments were approved by The University of Pennsylvania Institutional Animal Care and Use Committee.

Timed matings and handling of late gestation embryos. Overnight timed matings were set up using *Ccbe1*$^{+/-}$ and *Vegfr3*$^{kd/+}$ animals. Embryos from these crosses were collected at E16.5, E17.5, E18.5, and E19.5. Naturally born embryos were monitored for 1 h before sacrifice and tissue harvest. C-sections were performed at E19.5, during which embryos were removed from the uterus rapidly, stimulated manually, and monitored for 1 h. After 1 h, the lungs were collected for histology or lung dissection for testing flotation and wet to dry measurements. To examine prenatal lung morphology and development before air exposure and extra-uterine respiratory changes, the embryos were sacrificed in utero by immersing the gravid uterus in ice-cold PBS for 45 min before harvesting the embryos from the uterus under fluid. Prenatal whole chests and lungs were used for histology, transmission electron microscopy, phospholipid, DNA content, and compliance measurements.

Histological procedures and immunohistochemistry. Embryos and tissues were fixed in 10% formalin overnight, dehydrated in 100% ethanol, and embedded in paraffin. 8-µm-thick sections were used for hematoxylin-eosin, periodic acid-Schiff (PAS), trichrome, and immunohistochemistry staining. The following primary antibodies were used for immunostaining: anti-LYVE1 (R&D Systems), anti-PROX1 (Abcam), anti-PECAM1 (R&D Systems; clone: 693102), anti–pro-surfactant protein C (pro-SPC; EMD Millipore), anti-Clara cell 10 (CC10; Santa Cruz Biotechnology, Inc.), anti-Podoplanin (Abcam), anti–Caveolin-1 (BD), anti-PDGFRα (Cell Signaling Technology), anti-PDGFRβ (Cell Signaling Technology), anti-SM22α (Abcam), anti-WT1 (Santa Cruz Biotechnology, Inc.), anti-Vimentin (Santa Cruz Biotechnology, Inc.), anti-Desmin (Dako), and anti-NG2 (EMD Millipore). Detailed histology procedures can be found on the University of Pennsylvania Molecular Cardiology Research Center Histology and Gene Expression Core website. Microscopic images were taken on a microscope (Eclipse 80i; Nikon) connected to a camera (DS-Ri1; Nikon). Alveolar wall thickness (averaging 50–100 measurements per embryo) and alveolar area (averaging the total alveolar area in 5–15 vision fields per embryo) were performed in Elements software (Nikon) using a 40× objective.

Gene expression analysis. Quantitative real-time PCR analysis was used to measure the expression of late lung developmental markers in *Ccbe1*$^{-/-}$ and control embryos at E18.5. Total RNA was isolated with RNeasy micro kit (QIAGEN) followed by reverse transcription at 42°C for 50 min from 1 µg total RNA using the Superscript II Reverse transcription (Invitrogen). Real-time PCR was performed in

Power SYBR Green PCR Master Mix (Applied Biosciences) using the following primers: Sftpa1 forward, 5′-TGCACCTGGAGAACATGGAGACAA-3′; Sftpa1 reverse, 5′-ATGGATCCTTGCAAGCTGAGGACT-3′; Sftpb1 forward, 5′-TAGCCCTCTGCAGTGCTTCCAAA-3′; Sftpb1 reverse, 5′-AGCTGGGACATACAGACTGACACA-3′; Sftpc1 forward, 5′-ACCCTGTGTGGAGAGCTACCA-3′; Sftpc1 reverse, 5′-TTTGCGGAGGGTCTTTCCT-3′; Aqp5 forward, 5′-ATGAACCCAGCCCGATCTTT-3′; Aqp5 reverse, 5′-ACGATCGGTCCTACCCAGAAG-3′; Napsa forward, 5′-TCTAGTCCCCAGAGATGTCG-3′; Napsa reverse, 5′-AAGGTGGATTCGTTGAAGAGG-3′; Scgb1a1 forward, 5′-CCAACCTCTACCATGAAGATCG-3′; Scgb1a1 reverse, 5′-GGATGCCACATAACCAGACTC-3′; Foxj1 forward, 5′-CTTCTTCCAGAACCTTCCTCTG-3′; Foxj1 reverse, 5′-CACAGTCTCCAGAACACTCAC-3′; Tagln forward, 5′-TGGGAGCGAAATGTAACTGG-3′; Tagln reverse, 5′-GGGATCTGGGTCATTAGAGTTG-3′; Acta2 forward, 5′-ACTGGGACGACATGGAAAAG-3′; Acta2 reverse, 5′-AGGTCTCAAACATAATCTGGGTC-3′; Pdpn forward, 5′-GGAGGGCTTAATGAATCTACTGG-3′; Pdpn reverse, 5′-GGTTGTACTCTCGTGTTCTCTG-3′; Abca3 forward, 5′-CCTGTCTCCTATCTAATGTTGCC-3′; Abca3 reverse, 5′-TTGTCCAAAGCAGAAATTGTCG-3′; Ccbe1 forward, 5′-GCTCTGAAAACAAGATCACCACGAC-3′; and Ccbe1 reverse, 5′-GTACGGTCTCTCCCGCTTTTG-3′.

Trans-uterine echocardiography. Pregnant females were anesthetized with isoflurane and kept warm on a heating pad in the Mouse Cardiovascular Physiology and Microsurgery Core, University of Pennsylvania School of Medicine. Intrauterine echocardiography was performed using a Vevo 770 VisualSonic high resolution in vivo micro-imaging system. Heart morphology and function (ejection fraction and fractional shortening) of *Ccbe1*$^{-/-}$ and control embryos were analyzed at E18.5 as previously described (Lee et al., 2006).

Transmission electron microscopy. *Ccbe1*$^{-/-}$ and control E19.5 lungs were fixed with 2.5% glutaraldehyde, 2.0% paraformaldehyde in 0.1 M sodium cacodylate buffer, pH 7.4, overnight at 4°C followed by post-fixing in 2.0% osmium tetroxide dehydration. En bloc staining was performed with 2% uranyl acetate. After dehydration, the tissue was infiltrated and embedded in EMbed-812 (Electron Microscopy Sciences). Thin sections were stained with uranyl acetate and lead citrate and analyzed with an electron microscope (1010; JEOL) operated at 80 kV equipped with a digital camera (Hamamatsu) and image capture software (Advantage; AMT) in the Electron Microscopy Resource Laboratory of the University of Pennsylvania School of Medicine to show the presence of alveolar surfactant, the structure of the alveolar septal wall, and the morphology of type II and type I pneumocytes.

Lung flotation and wet/dry (W/D) ratio. Explanted *Ccbe1*$^{-/-}$, *Vegfr3*$^{kd/kd}$, and control lungs were placed into 500 µl of fluid 60 min after the C-section, and flotation was documented. For the W/D ratio measurements, lungs were harvested from *Ccbe1*$^{-/-}$ and control embryos 60 min after C-section to obtain wet weight, and then placed into a DNA SpeedVac (Savant) for 4 h to obtain dry weight.

Lung phospholipid protein ratio and DNA content measurements. For lung phospholipid protein ratio measurements *Ccbe1*$^{-/-}$ and control E19.5 embryos were rapidly dissected, and the left lungs were frozen in liquid N_2 followed by homogenization in distilled water. The homogenates were analyzed for protein content using Lowry's method. Afterward, lipids were extracted from the samples with chloroform–methanol followed by phospholipid analysis (Atochina-Vasserman et al., 2011).

Total DNA content was isolated from the left lungs of *Ccbe1*$^{-/-}$ and control E18.5 embryos using a DNeasy blood and tissue kit (QIAGEN). DNA concentration of the samples was determined by a NanoDrop 1000 system (Thermo Fisher Scientific).

Prenatal pulmonary lymphangiography. To test lymphatic function in the prenatal lung, 20 µl of 70 kD tetramethylrhodamine-dextran (TMR-dextran; Invitrogen) at 10 mg/ml concentration was injected through the uterine and chest walls into the lungs of live *Prox1*^{GFP} transgenic embryos at E18.5 and E17.5. Selective uptake and passage of rhodamine-dextran in GFP positive lymphatic vessels was detected 45 min after the injections. The embryonic lungs were removed and imaged under a fluorescent research stereomicroscope (SZX16; Olympus) equipped with a camera system (DP72; Olympus).

Compliance measurements. The custom set-up to measure lung compliance consisted of a PBS reservoir attached via flexible tubing to a long glass capillary tube that was mounted horizontally. The other end of the capillary tube was pulled to form a microneedle. The entire system was flushed with PBS to remove any air and a small droplet of vegetable oil was placed in the capillary tube as a fiducial marker. Explanted E18.5 *Ccbe1*$^{-/-}$, *Vegfr3*$^{kd/kd}$, and control lungs were intubated with a microneedle and secured with a modified finger trap suture. Lung transmural pressure was changed by adjusting the reservoir height to alter the lumenal pressure applied to the explants. Lung volume change was calculated by measuring the displacement of the oil drop in the capillary tube (ΔL) and multiplying by the cross-sectional area of the capillary tube ($\pi/4*ID^2$). Several inflation and deflation cycles were performed and data were collected at several pressures over a single inflation and deflation cycle. Compliance was calculated as the slope of the pressure-volume curve.

Presentation of data and statistical analysis. Macroscopic pictures and microscopic images are representative of three or more independent experiments. Microscopic image processing and analysis were performed using Photoshop (Adobe) and Fiji software (National Institutes of Health). Results are shown as mean and SEM. Statistical analyses were performed using Student unpaired two-tailed *t* test or χ^2 analysis using Prism 5 software. A difference was considered statistically significant at $P < 0.05$.

Online supplemental material. Video 1 shows that *Ccbe1*$^{-/-}$ neonates are born alive and exhibit normal respiratory movements. Video 2 shows that *Vegfr3*$^{kd/kd}$ neonates are born alive and exhibit normal respiratory movements. Online supplemental material is available at http://www.jem.org/cgi/content/full/jem.20132308/DC1.

The authors thank Ed Morrisey, Tien Peng, Michael Beers, and the members of the Kahn laboratory for valuable discussions and insights during the course of these studies. We thank Veerpal Dhillon and Mei Chen for technical assistance.

This work was supported by HL103432 and by the Leducq Foundation (M.L. Kahn), and by HL110335 (C.M. Nelson).

The authors declare no competing financial interests.

Submitted: 4 November 2013
Accepted: 19 March 2014

REFERENCES

Adams, F.H., T. Fujiwara, G. Emmanouilides, and A. Scudder. 1965. Surface properties and lipids from lungs of infants with hyaline membrane disease. *J. Pediatr.* 66:357–364. http://dx.doi.org/10.1016/S0022-3476(65)80193-7

Alders, M., B.M. Hogan, E. Gjini, F. Salehi, L. Al-Gazali, E.A. Hennekam, E.E. Holmberg, M.M. Mannens, M.F. Mulder, G.J. Offerhaus, et al. 2009. Mutations in CCBE1 cause generalized lymph vessel dysplasia in humans. *Nat. Genet.* 41:1272–1274. http://dx.doi.org/10.1038/ng.484

Atochina-Vasserman, E.N., S.R. Bates, P. Zhang, H. Abramova, Z. Zhang, L. Gonzales, J.Q. Tao, B.R. Gochuico, W. Gahl, C.J. Guo, et al. 2011. Early alveolar epithelial dysfunction promotes lung inflammation in a mouse model of Hermansky-Pudlak syndrome. *Am. J. Respir. Crit. Care Med.* 184:449–458. http://dx.doi.org/10.1164/rccm.201011-1882OC

Avery, M.E., and J. Mead. 1959. Surface properties in relation to atelectasis and hyaline membrane disease. *AMA J. Dis. Child.* 97:517–523.

Bellini, C., M. Mazzella, C. Arioni, C. Campisi, G. Taddei, P. Tomà, F. Boccardo, R.C. Hennekam, and G. Serra. 2003. Hennekam syndrome presenting as nonimmune hydrops fetalis, congenital chylothorax, and congenital pulmonary lymphangiectasia. *Am. J. Med. Genet. A.* 120A:92–96. http://dx.doi.org/10.1002/ajmg.a.20180

Bland, R.D., T.N. Hansen, C.M. Haberkern, M.A. Bressack, T.A. Hazinski, J.U. Raj, and R.B. Goldberg. 1982. Lung fluid balance in lambs before and after birth. *J. Appl. Physiol.* 53:992–1004.

Bourbon, J.R., M. Rieutort, M.J. Engle, and P.M. Farrell. 1982. Utilization of glycogen for phospholipid synthesis in fetal rat lung. *Biochim. Biophys. Acta.* 712:382–389. http://dx.doi.org/10.1016/0005-2760(82)90356-3

Clark, J.C., T.E. Weaver, H.S. Iwamoto, M. Ikegami, A.H. Jobe, W.M. Hull, and J.A. Whitsett. 1997. Decreased lung compliance and air trapping in heterozygous SP-B-deficient mice. *Am. J. Respir. Cell Mol. Biol.* 16:46–52. http://dx.doi.org/10.1165/ajrcmb.16.1.8998078

Compernolle, V., K. Brusselmans, T. Acker, P. Hoet, M. Tjwa, H. Beck, S. Plaisance, Y. Dor, E. Keshet, F. Lupu, et al. 2002. Loss of HIF-2alpha and inhibition of VEGF impair fetal lung maturation, whereas treatment with VEGF prevents fatal respiratory distress in premature mice. *Nat. Med.* 8:702–710. http://dx.doi.org/10.1038/nm1102-1329b

Couser, R.J., T.B. Ferrara, J. Ebert, R.E. Hoekstra, and J.J. Fangman. 1990. Effects of exogenous surfactant therapy on dynamic compliance during mechanical breathing in preterm infants with hyaline membrane disease. *J. Pediatr.* 116:119–124. http://dx.doi.org/10.1016/S0022-3476(05)81660-9

Guyton, A.C., and J.E. Hall. 2000. Textbook of Medical Physiology. W.B. Saunders Company: Philadelphia. 1120 pp.

Haddy, T.B., and F.J. Haddy. 1964. The Effect of acute pulmonary edema upon lung compliance. *Pediatrics.* 33:55–62.

Hintz, S.R., W.K. Poole, L.L. Wright, A.A. Fanaroff, D.E. Kendrick, A.R. Laptook, R. Goldberg, S. Duara, B.J. Stoll, and W. Oh; NICHD Neonatal Research Network. 2005. Changes in mortality and morbidities among infants born at less than 25 weeks during the post-surfactant era. *Arch. Dis. Child. Fetal Neonatal Ed.* 90:F128–F133. http://dx.doi.org/10.1136/adc.2003.046268

Hummler, E., P. Barker, J. Gatzy, F. Beermann, C. Verdumo, A. Schmidt, R. Boucher, and B.C. Rossier. 1996. Early death due to defective neonatal lung liquid clearance in αENaC-deficient mice. *Nat. Genet.* 12: 325–328. http://dx.doi.org/10.1038/ng0396-325

Janér, J., P. Lassus, C. Haglund, K. Paavonen, K. Alitalo, and S. Andersson. 2006. Pulmonary vascular endothelial growth factor-C in development and lung injury in preterm infants. *Am. J. Respir. Crit. Care Med.* 174:326–330. http://dx.doi.org/10.1164/rccm.200508-1291OC

Kaipainen, A., J. Korhonen, T. Mustonen, V.W. van Hinsbergh, G.H. Fang, D. Dumont, M. Breitman, and K. Alitalo. 1995. Expression of the fms-like tyrosine kinase 4 gene becomes restricted to lymphatic endothelium during development. *Proc. Natl. Acad. Sci. USA.* 92:3566–3570. http://dx.doi.org/10.1073/pnas.92.8.3566

Karkkainen, M.J., A. Saaristo, L. Jussila, K.A. Karila, E.C. Lawrence, K. Pajusola, H. Bueler, A. Eichmann, R. Kauppinen, M.I. Kettunen, et al. 2001. A model for gene therapy of human hereditary lymphedema. *Proc. Natl. Acad. Sci. USA.* 98:12677–12682. http://dx.doi.org/10.1073/pnas.221449198

Karkkainen, M.J., P. Haiko, K. Sainio, J. Partanen, J. Taipale, T.V. Petrova, M. Jeltsch, D.G. Jackson, M. Talikka, H. Rauvala, et al. 2004. Vascular endothelial growth factor C is required for sprouting of the first lymphatic vessels from embryonic veins. *Nat. Immunol.* 5:74–80. http://dx.doi.org/10.1038/ni1013

Kobayashi, K., R.P. Lemke, and J.J. Greer. 2001. Ultrasound measurements of fetal breathing movements in the rat. *J. Appl. Physiol.* 91:316–320.

Kulkarni, R.M., A. Herman, M. Ikegami, J.M. Greenberg, and A.L. Akeson. 2011. Lymphatic ontogeny and effect of hypoplasia in developing lung. *Mech. Dev.* 128:29–40. http://dx.doi.org/10.1016/j.mod.2010.09.003

Laurence, K.M. 1955. Congenital pulmonary cystic lymphangiectasis. *J. Pathol. Bacteriol.* 70:325–331. http://dx.doi.org/10.1002/path.1700700208

Lee, J.S., Q. Yu, J.T. Shin, E. Sebzda, C. Bertozzi, M. Chen, P. Mericko, M. Stadtfeld, D. Zhou, L. Cheng, et al. 2006. Klf2 is an essential regulator of vascular hemodynamic forces in vivo. *Dev. Cell.* 11:845–857. http://dx.doi.org/10.1016/j.devcel.2006.09.006

Mäkinen, T., T. Veikkola, S. Mustjoki, T. Karpanen, B. Catimel, E.C. Nice, L. Wise, A. Mercer, H. Kowalski, D. Kerjaschki, et al. 2001. Isolated lymphatic endothelial cells transduce growth, survival and migratory signals via the VEGF-C/D receptor VEGFR-3. *EMBO J.* 20:4762–4773. http://dx.doi.org/10.1093/emboj/20.17.4762

Martel, C., W. Li, B. Fulp, A.M. Platt, E.L. Gautier, M. Westerterp, R. Bittman, A.R. Tall, S.H. Chen, M.J. Thomas, et al. 2013. Lymphatic vasculature mediates macrophage reverse cholesterol transport in mice. *J. Clin. Invest.* 123:1571–1579. http://dx.doi.org/10.1172/JCI63685

Milner, A.D., and R.A. Sauders. 1977. Pressure and volume changes during the first breath of human neonates. *Arch. Dis. Child.* 52:918–924. http://dx.doi.org/10.1136/adc.52.12.918

Moessinger, A.C., R. Harding, T.M. Adamson, M. Singh, and G.T. Kiu. 1990. Role of lung fluid volume in growth and maturation of the fetal sheep lung. *J. Clin. Invest.* 86:1270–1277. http://dx.doi.org/10.1172/JCI114834

Morgan, T.E. 1971. Pulmonary surfactant. *N. Engl. J. Med.* 284:1185–1193. http://dx.doi.org/10.1056/NEJM197105272842105

Morikawa, S., P. Baluk, T. Kaidoh, A. Haskell, R.K. Jain, and D.M. McDonald. 2002. Abnormalities in pericytes on blood vessels and endothelial sprouts in tumors. *Am. J. Pathol.* 160:985–1000. http://dx.doi.org/10.1016/S0002-9440(10)64920-6

Nogee, L.M., G. Garnier, H.C. Dietz, L. Singer, A.M. Murphy, D.E. deMello, and H.R. Colten. 1994. A mutation in the surfactant protein B gene responsible for fatal neonatal respiratory disease in multiple kindreds. *J. Clin. Invest.* 93:1860–1863. http://dx.doi.org/10.1172/JCI117173

Noonan, J.A., L.R. Walters, and J.T. Reeves. 1970. Congenital pulmonary lymphangiectasis. *Am. J. Dis. Child.* 120:314–319.

Patrick, J., and J. Challis. 1980. Measurement of human fetal breathing movements in healthy pregnancies using a real-time scanner. *Semin. Perinatol.* 4:275–286.

Schnitzer, J., W.W. Franke, and M. Schachner. 1981. Immunocytochemical demonstration of vimentin in astrocytes and ependymal cells of developing and adult mouse nervous system. *J. Cell Biol.* 90:435–447. http://dx.doi.org/10.1083/jcb.90.2.435

Sharp, J.T., G.T. Griffith, I.L. Bunnell, and D.G. Greene. 1958. Ventilatory mechanics in pulmonary edema in man. *J. Clin. Invest.* 37:111–117. http://dx.doi.org/10.1172/JCI103577

Suresh, G.K., and R.F. Soll. 2005. Overview of surfactant replacement trials. *J. Perinatol.* 25:S40–S44. http://dx.doi.org/10.1038/sj.jp.7211320

Tammela, T., and K. Alitalo. 2010. Lymphangiogenesis: Molecular mechanisms and future promise. *Cell.* 140:460–476. http://dx.doi.org/10.1016/j.cell.2010.01.045

Wang, Y., and G. Oliver. 2010. Current views on the function of the lymphatic vasculature in health and disease. *Genes Dev.* 24:2115–2126. http://dx.doi.org/10.1101/gad.1955910

Wigle, J.T., and G. Oliver. 1999. Prox1 function is required for the development of the murine lymphatic system. *Cell.* 98:769–778. http://dx.doi.org/10.1016/S0092-8674(00)81511-1

Zhang, L., F. Zhou, W. Han, B. Shen, J. Luo, M. Shibuya, and Y. He. 2010. VEGFR-3 ligand-binding and kinase activity are required for lymphangiogenesis but not for angiogenesis. *Cell Res.* 20:1319–1331. http://dx.doi.org/10.1038/cr.2010.116

Zou, Z., D.R. Enis, H. Bui, E. Khandros, V. Kumar, Z. Jakus, C. Thom, Y. Yang, V. Dhillon, M. Chen, et al. 2013. The secreted lymphangiogenic factor CCBE1 is essential for fetal liver erythropoiesis. *Blood.* 121:3228–3236. http://dx.doi.org/10.1182/blood-2012-10-462689